

Three-phase adaptive reclosure for transmission lines with shunt reactors using mode current oscillation frequencies

Xinghua Huang¹ ✉, Guobing Song¹, Ting Wang¹, Yaobin Gu¹

¹School of Electrical Engineering, Xi'an Jiaotong University, Xi'an 710049, People's Republic of China

✉ E-mail: xhhuangxjtu@qq.com

Abstract: A three-phase adaptive reclosing scheme using mode current oscillation frequencies is proposed for transmission lines with shunt reactors. Firstly, with phase-mode transformation, the fault boundary conditions are analysed and then the composite mode networks are constructed, respectively, for transient faults and permanent faults. In the composite networks, mode currents of shunt reactors are computed and thus oscillation frequencies are obtained. It is found that in transient fault situations, mode currents oscillate in only one frequency which is the natural frequency of the corresponding mode network. By contrast, the number of frequency components varies in permanent fault situations, depending on the fault type. Based on the frequency characteristics discussed above, a three-phase adaptive reclosing scheme is conceived. In the scheme, the transient fault is identified only if the shunt reactor mode currents contain one frequency which is equal to the natural frequency of the corresponding mode network. Otherwise the fault is taken to be permanent. By simulation, the correctness of the frequency characteristics is verified and the reclosing scheme is validated, hardly affected by fault locations and fault resistance.

1 Introduction

Reclosure for transmission lines is widely used in power systems to ensure rapid recovery of power supply and to enhance the system stability in transient fault situations. However, in permanent fault situations, reclosure may aggravate potential damage to the equipment and the entire system [1, 2]. Therefore, it is of practical significance to detect the fault nature before reclosure by making use of adaptive reclosure [3].

Until now, single-phase adaptive reclosure [3–5] is studied comparatively further than three-phase adaptive reclosure [6–13]. The main advantage of single-phase adaptive reclosure over three-phase adaptive reclosure is that only the fault phase is interrupted when a single-phase fault occurs. The continuous operation of the rest two phases implies the continuous power supply and improved system reliability. However, as the power grid becomes increasingly robust and reliable due to infrastructure investment (especially in undeveloped areas), three-phase adaptive reclosure is likely to have a range of applications wider than today. Thus, it is essential to advance the studies on three-phase adaptive reclosure.

The existing schemes for three-phase adaptive reclosure can be generally divided into three categories. The first category identifies the fault nature based on the propagation characteristics of high-frequency signals in the carrier channel [6]. This method is unacceptable for power lines without high-frequency signal channels. In the second category, the characteristics of the recovery voltage are investigated, based on which the fault nature is detected [7, 8]. In many practical cases, however, extracting the voltage signal is difficult since the potential transformer is not installed. Moreover, the measurement precision is often an issue for potential transformers. The methods in the third category focus the currents in the shunt reactors [9–13]. In [9–12], it is demonstrated that in essence the difference between transient faults and permanent faults is the line topology. Accordingly, the fault nature can be decided by estimating the system parameters using the measured current data. However, for transmission lines with shunt reactors at both ends, the current data at both ends are required, which relies on a communications system. Besides, when the fault resistance is high, the methods in [9–12] might fail to make a right decision on fault nature. Detecting the fault nature using shunt reactor current frequencies is proposed in [13]. Using the current oscillation frequencies is quite a feasible scheme, since the oscillation frequencies are constant despite the current attenuation. However, a

quantitative analysis of the frequencies is not provided in [13]. In addition, only single-phase faults are concerned in [13].

Based on the studies carried out in [13], this paper goes on to investigate the current oscillation frequencies to facilitate three-phase adaptive reclosure. A comprehensive analysis of oscillation frequencies under different fault types is provided quantitatively. Then, according to the frequency characteristics, an adaptive reclosure scheme is proposed. Compared to existing schemes in [6–12], the proposed scheme is more applicable in an overall sense. Only the data at one end of the line is required, implying no need for communications channels. The current data, rather than the voltage data are used, which is easy to implement in practice. Besides, the feasibility of the proposed scheme is hardly affected by the fault location and fault resistance.

2 Analysis of mode network

The analysis of a system with shunt reactors at both ends is given below. When the shunt reactor is installed at only one end, the analysis methodology is exactly the same, which will be demonstrated later in this section.

Fig. 1 shows a system with shunt reactors at both ends (M-end and N-end), where the G_m and G_n denote the ac sources, Z_m and Z_n denote the source impedance, L_{pm} and L_{pn} denote the shunt reactors, and L_{qm} and L_{qn} denote the neutral reactors.

With phase-mode transformation, not only the interaction of three-phase quantities can be decoupled, also the transient state in time domain and frequency domain can be conveniently analysed. As a common phase-mode transformation, Karenbauer transformation [14] is used in this paper

$$[A_0, A_1, A_2]^T = T[A_a, A_b, A_c]^T \quad (1)$$

where T denotes the transformation matrix, A denotes a quantity such as current or voltage, A_0 , A_1 and A_2 denote the mode components of A , and A_a , A_b and A_c denote the phase components of A . T is expressed as follows:

$$T = \frac{1}{3} \begin{bmatrix} 1 & 1 & 1 \\ 1 & -1 & 0 \\ 1 & 0 & -1 \end{bmatrix} \quad (2)$$

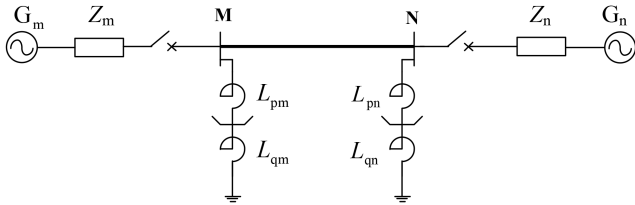


Fig. 1 System with shunt reactors at both ends

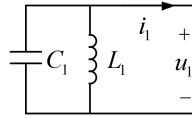


Fig. 2 1-mode network after three-phase trip

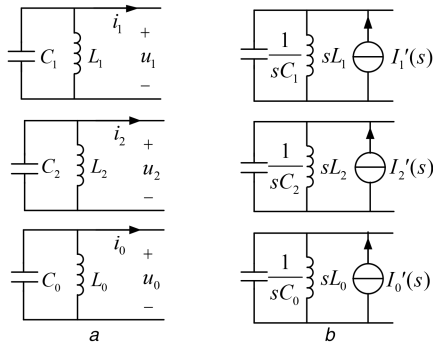


Fig. 3 Composite mode network in transient fault situations

(a) Time-domain network, (b) Frequency-domain network

Since the line reactance is much smaller than the shunt reactance, it can be reasonably disregarded in the mode network. After the three-phase trip at both ends, the 1-mode network is depicted in Fig. 2, where i_1 and u_1 are the 1-mode current and voltage at the fault point, respectively, C_1 is the equivalent 1-mode line capacitance, and L_1 is the equivalent 1-mode reactance of shunt reactors.

The structures of the 2-mode and 0-mode networks are the same as the 1-mode network in Fig. 2. The only difference is the value of network parameters. Supposing that the shunt reactance is identical for both ends of the transmission line, we have

$$L_1 = L_2 = L_{pm}/2, \quad L_0 = (L_{pm} + 3L_{qm})/2 \quad (3)$$

For transmission lines with shunt reactors at only one end, after three-phase trip at both ends, the 1-mode, 2-mode and 0-mode network structures are the same as in Fig. 2. The corresponding reactance is

$$L_1 = L_2 = L_{pm}, \quad L_0 = L_{pm} + 3L_{qm} \quad (4)$$

3 Analysis of mode current frequencies

After the three-phase trip following a transient fault or permanent fault, the fault boundary conditions can be derived in mode domain using (1). Then, the interconnection of 1-mode, 2-mode and 0-mode networks can be analysed to obtain the composite mode networks. In the composite network, the shunt reactor current is investigated regarding the oscillation frequencies.

3.1 Transient fault situation

After arc extinction at the fault point, the fault boundary condition can be expressed as (5)

$$i_a = i_b = i_c = 0 \quad (5)$$

Using (1), the boundary condition in (5) can be re-written in the mode domain

$$i_0 = i_1 = i_2 = 0 \quad (6)$$

Equation (6) shows that the mode currents at the fault point are zero. Therefore, the 1-mode, 2-mode and 0-mode networks are all open circuits. Put differently, the 1-mode, 2-mode and 0-mode networks are disconnected from each other, as shown in Fig. 3a.

Fig. 3b shows the frequency-domain circuit corresponding to Fig. 3a. In Fig. 3b, $I'_i(s)$ ($i = 1, 2, 0$) designates the current source generated by the initial state of the capacitor and reactor. The form of $I'_i(s)$ is $\alpha_i + (\beta_i/s)$, where α_i and β_i are decided by the initial state of the capacitor and reactor.

According to Fig. 3b, the shunt reactor mode currents $I_{L1}(s)$, $I_{L2}(s)$, $I_{L0}(s)$ are obtained as follows:

$$\begin{cases} I_{L1}(s) = \frac{\alpha_1 s + \beta_1}{s(s^2 L_1 C_1 + 1)} \\ I_{L2}(s) = \frac{\alpha_2 s + \beta_2}{s(s^2 L_2 C_2 + 1)} \\ I_{L0}(s) = \frac{\alpha_0 s + \beta_0}{s(s^2 L_0 C_0 + 1)} \end{cases} \quad (7)$$

By analysing the denominators in (7), the mode current oscillation frequencies are computed as follows:

$$\begin{cases} f_{11} = \frac{1}{2\pi} \sqrt{\frac{1}{L_1 C_1}} \\ f_{21} = \frac{1}{2\pi} \sqrt{\frac{1}{L_2 C_2}} = f_{11} \\ f_{01} = \frac{1}{2\pi} \sqrt{\frac{1}{L_0 C_0}} \end{cases} \quad (8)$$

where f_{ij} denotes the j th oscillation frequency of the i -mode current ($i = 1, 2, 0$ and $j = 1, 2, 3, \dots$).

Equation (8) demonstrates that each of the 1-mode, 2-mode and 0-mode currents oscillates in only one frequency which is the natural frequency of the corresponding mode network.

3.2 Permanent fault situation

Here, the phase B to ground fault is taken as the example. The boundary condition for permanent phase B to ground fault is

$$\begin{cases} u_b = 0 \\ i_a = i_c = 0 \end{cases} \quad (9)$$

Transforming (9) into mode quantities using (1), we obtain

$$\begin{cases} u_0 - 2u_1 + u_2 = 0 \\ i_0 + i_1 = 0 \\ i_2 = 0 \end{cases} \quad (10)$$

The composite mode network which complies with the relation in (10) is presented in Fig. 4a. Fig. 4b shows the corresponding network in frequency domain.

Deduced in Fig. 4b, the shunt reactor currents are as follows: (see (11)) Accordingly, the mode current oscillation frequencies are derived by analysing the denominators in (11)

$$\begin{cases} f_{11} = \frac{1}{2\pi} \sqrt{\frac{1}{L_1 C_1}}, \quad f_{12} = \frac{1}{2\pi} \sqrt{\frac{2L_1 + L_0}{L_0 L_1 (2C_0 + C_1)}} \\ f_{21} = \frac{1}{2\pi} \sqrt{\frac{1}{L_2 C_2}} = f_{11} \\ f_{01} = \frac{1}{2\pi} \sqrt{\frac{2L_1 + L_0}{L_0 L_1 (2C_0 + C_1)}} \end{cases} \quad (12)$$

Seen from (12), there are two oscillation components in the 1-mode current whereas there is only one oscillation component in the 2-mode or 0-mode current.

The methodology for analysing other fault types is exactly the same. That is, with mode domain fault boundary conditions, the composite mode network can be constructed, in which the shunt reactor mode currents and the oscillation frequencies can then be figured out. Table 1 summarises the oscillation frequencies under all fault types. In this table, the notations A, B and C signify the fault phases, G signifies grounded faults. For example, AG denotes phase A to ground fault and AB denotes phase A-phase B ungrounded fault. The notation ‘\’ signifies that there is no oscillation component, and f_1 , f_0 , f_p and f_q signify the following values:

$$\begin{cases} f_1 = \frac{1}{2\pi} \sqrt{\frac{1}{L_1 C_1}} \\ f_0 = \frac{1}{2\pi} \sqrt{\frac{1}{L_0 C_0}} \end{cases} \begin{cases} f_p = \frac{1}{2\pi} \sqrt{\frac{2L_1 + L_0}{L_0 L_1 (2C_0 + C_1)}} \\ f_q = \frac{1}{2\pi} \sqrt{\frac{2L_0 + L_1}{L_0 L_1 (2C_1 + C_0)}} \end{cases} \quad (13)$$

It should be noted that the result in Table 1 also applies to transmission systems with shunt reactors at only one end, since the mode network structure is the same as that of a system with shunt reactors at both ends.

3.3 Impact of the fault resistance

The impact of the fault resistance is discussed in this subsection as it is not taken into account in Sections 3.1 and 3.2.

If a transient fault occurs with a fault resistance, the boundary condition after arc extinction can still be expressed in (5). Therefore, the composite mode network remains the same as shown in Fig. 3, implying that the oscillation frequencies are still the results in (8).

To investigate the permanent fault with a fault resistance R_f , the discussion on phase B to ground fault is demonstrated here. The fault boundary condition is

$$\begin{cases} u_b = R_f i_b \\ i_a = i_c = 0 \end{cases} \quad (14)$$

Transformed into the mode domain, (14) is re-written as

$$\begin{cases} u_0 - 2u_1 + u_2 = 3R_f i \\ i_0 + i_1 = 0 \\ i_2 = 0 \end{cases} \quad (15)$$

There is a series resistor in the composite mode network deduced in (15), which is the only difference from the composite mode network in Fig. 4 deduced in (10). The series resistor $3R_f$ is depicted in grey-dotted line in Fig. 4. In fact, the analysis of other fault types also shows that the fault resistance behaves as a series resistance in the composite mode network. It is true that the theoretical expressions of shunt reactor currents would get complicated by R_f . However, during the transient state of a circuit, the main impact of the series resistance is energy attenuation. The oscillation frequencies, which are decided mainly by capacitance and reactance, are hardly influenced by R_f . Therefore, the result in Table 1 still holds true when the fault is not metallic.

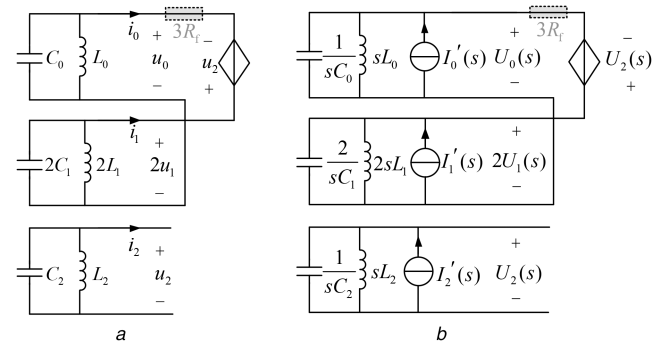


Fig. 4 Composite mode network in permanent phase B to ground fault situations

(a) Time-domain network, (b) Frequency-domain network

Table 1 Oscillation frequencies of shunt reactor mode currents under different fault types

Fault type	Oscillation frequency		
	1-mode	2-mode	0-mode
transient fault	f_1	f_1	f_0
permanent fault	AG	f_1, f_p	f_p
	BG	f_1, f_p	f_p
	CG	f_1	f_p
	AB	\	f_0
	AC	f_1	\
	BC	f_1	f_0
	ABG	\	f_q
	ACG	f_q	\
	BCG	f_q	f_q
	ABC	\	f_0
	ABCG	\	\

4 Three-phase adaptive reclosure scheme

Table 1 exhibits that the transient faults are distinct from the permanent faults in terms of the mode current frequencies. The only exception is that under phase B–phase C ungrounded fault situations, the frequencies in Table 1 fail to distinguish the fault nature.

It is worth noting that the phase-mode transformation in (2) calculates the 1-mode component with phases A and B, and calculates the 2-mode component with phases A and C. If the columns in (2) are exchanged to obtain the new matrix as

$$T' = \frac{1}{3} \begin{bmatrix} 1 & 1 & 1 \\ 0 & 1 & -1 \\ -1 & 1 & 0 \end{bmatrix} \quad (16)$$

where the 1-mode component is now calculated with phases B and C, and the 2-mode component is now calculated with phases B and A, then the mode current frequencies for permanent phase B-phase C ungrounded faults will be exactly those for permanent phase A-phase B ungrounded faults in Table 1.

Therefore, to distinguish the fault nature, whether to use the transformation matrix in (16) or (2) is based on fault phase selection action. If the matrix in (16) is used in phase B–phase C

$$\begin{cases} I_{L1}(s) = \frac{(s^2 C_0 + (1/L_0))(\alpha_2 s + \beta_2)(\alpha_1 + \alpha_0)s + (\beta_1 + \beta_0)}{2sL_1[s^2((C_1/2) + C_0) + ((1/2L_1) + (1/L_0))](s^2 C_2 + (1/L_2))} \\ I_{L2}(s) = \frac{\alpha_2 + \beta_2}{s(s^2 L_2 C_2 + 1)} \\ I_{L0}(s) = \frac{(\alpha_1 + \alpha_0 - (1/2)\alpha_2)s + (\beta_1 + \beta_0 - (1/2)\beta_2)}{sL_0[s^2((C_1/2) + C_0) + ((1/2L_1) + (1/L_0))]} \end{cases} \quad (11)$$

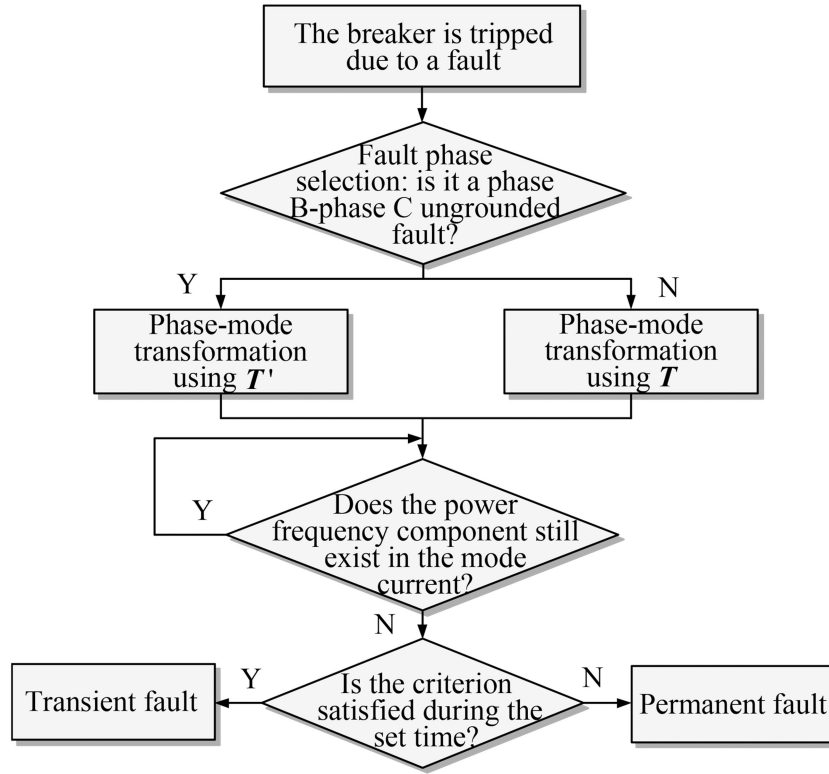


Fig. 5 Flow chart of the reclosure scheme

ungrounded faults and the matrix in (2) is used in other fault types, then the fault nature can be properly identified.

According to the frequency characteristics discussed above, the criterion to identify a transient fault is stated as: each of the 1-mode, 2-mode and 0-mode currents of the shunt reactor must contain only one oscillation frequency, and the frequency must satisfy

$$\begin{cases} |f_{1_measured} - f_1| < \lambda \\ |f_{2_measured} - f_1| < \lambda \\ |f_{0_measured} - f_0| < \lambda \end{cases} \quad (17)$$

where $f_{1_measured}$, $f_{2_measured}$ and $f_{0_measured}$ represent the measured 1-mode, 2-mode and 0-mode frequencies, respectively, and λ represents the permissible measurement error. Once the criterion is not satisfied, the fault is considered to be permanent.

The proposed scheme works independent of communications between both ends of the transmission line. Only the data at the local end is needed. In this scheme, the frequency measurement starts when the circuit breaker is tripped at the local end. As long as the breaker is not tripped at either end, the power frequency component would be measured in the local mode current, since the ac source is not disconnected yet. Put differently, the power frequency component vanishes only when the circuit is open at both ends. Therefore, the moment the power frequency component vanishes is the moment the criterion starts to identify the fault nature. During the set time for fault nature identification, if the fault is transient, the measured frequencies would meet the criterion from the moment of arc extinction. By contrast, if the fault is permanent, the measured frequencies would fail to meet the criterion all the time. The flow chart of the scheme is presented in Fig. 5.

5 Validation by simulation

In PSCAD, a transmission system is built with shunt reactors at both ends or at a single end. The rated voltage is 500 kV and the rated frequency is 50 Hz. The other parameters are as follows:

(a) AC source sequence parameters: $Z_{m_1} = Z_{m_2} = 49.36 \Omega$, $Z_{m_0} = 41.34 \Omega$, $Z_{n_1} = Z_{n_2} = 46.03 \Omega$, $Z_{n_0} = 103.36 \Omega$;

(b) Line sequence parameters: Bergeron model, line length is 358 km, $R_{line_1} = R_{line_2} = 19.5 \text{ m}\Omega/\text{km}$, $R_{line_0} = 167.5 \text{ m}\Omega/\text{km}$, $L_{line_1} = L_{line_2} = 913.4 \mu\text{H}/\text{km}$, $L_{line_0} = 2.739 \text{ mH}/\text{km}$, $C_{line_1} = C_{line_2} = 14 \text{ nF}/\text{km}$, $C_{line_0} = 3.5 \text{ nF}/\text{km}$;

(c) Shunt reactance: $L_{pm} = L_{pn} = 15.35 \text{ H}$;

(d) Neutral reactance: $L_{qm} = L_{qn} = 1.38 \text{ H}$.

The matrix pencil method [15] is used in this paper to extract the mode current frequencies. With the element parameters given above, the theoretical oscillation frequencies can be computed using (13). That is, if the shunt reactor is at a single end, $f_1 = 18.15 \text{ Hz}$, $f_0 = 32.20 \text{ Hz}$, $f_p = 23.77 \text{ Hz}$, $f_q = 20.20 \text{ Hz}$; if the shunt reactors are at both ends, $f_1 = 25.66 \text{ Hz}$, $f_0 = 45.54 \text{ Hz}$, $f_p = 33.62 \text{ Hz}$, $f_q = 28.56 \text{ Hz}$.

In the reclosure scheme, $\lambda = 2 \text{ Hz}$, and the set time for fault nature identification is 0.2 s.

5.1 Simulation results when the reactor is at a single end

Due to limited space, the phase C to ground fault is taken as the example. The simulation results are provided in Table 2, in which the fault distance is the percentage of line length away from the M-end of the line. Table 2 is consistent with the theoretical result in Table 1, regardless of the fault location and fault resistance.

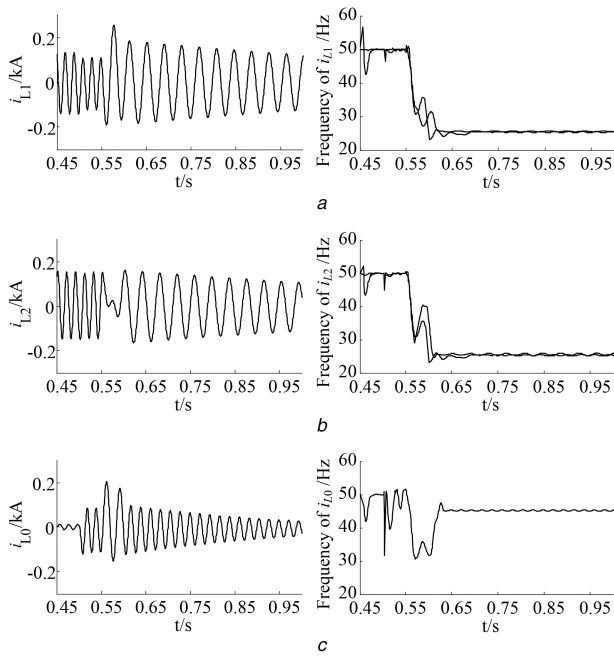
5.2 Simulation results when the reactors are at both ends

5.2.1 Transient faults: In the simulation scenario, a phase A to ground fault occurs with the fault resistance $R_f = 300 \Omega$. The fault point is 200 km away from the M-end of the line. The fault occurs at 0.45 s. The M-end and N-end breakers are tripped, respectively, at 0.5 and 0.55 s. The arc extinction takes place at 0.6 s. The M-end shunt reactor mode currents and oscillation frequencies are exhibited in Fig. 6, in which i_{L1} , i_{L2} and i_{L0} represent the 1-mode, 2-mode and 0-mode currents, respectively.

Seen from Fig. 6, before the circuit is open at both ends at 0.55 s, the power frequency (50 Hz) is obvious in i_{L1} and i_{L2} . After the arc extinction at 0.6 s, each of i_{L1} , i_{L2} and i_{L0} oscillates in only one

Table 2 Simulation results of phase C to ground faults

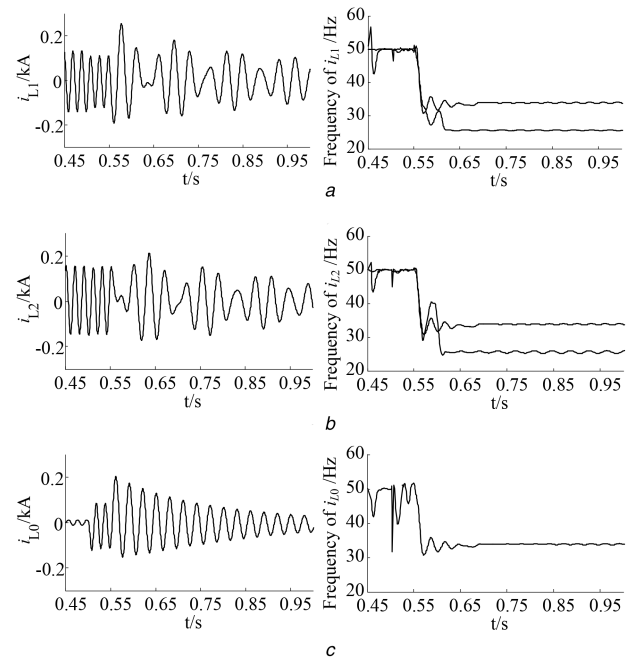
Fault distance, %	R_f, Ω	Frequencies under transient faults, Hz			Frequencies under permanent faults, Hz		
		1-mode	2-mode	0-mode	1-mode	2-mode	0-mode
0	0	18.01	17.95	31.73	18.01	18.01	23.26
						23.30	
	300	18.00	17.97	31.74	18.00	18.01	23.31
25	0	18.06	18.03	31.85	18.06	18.05	23.48
						23.46	
	300	18.05	18.05	31.83	18.03	18.05	23.47
50	0	18.06	18.09	31.93	18.06	18.10	23.61
						23.58	
	300	18.08	18.10	31.90	18.11	18.08	23.60
75	0	18.08	18.07	31.91	18.10	18.08	23.61
						23.60	
	300	18.06	18.06	31.91	18.09	18.09	23.58
100	0	18.01	18.00	31.80	18.04	18.03	23.32
						23.32	
	300	18.02	17.97	31.83	18.01	17.98	23.25
						23.28	

**Fig. 6** M-end mode currents and the frequencies under a transient phase A to ground fault(a) i_{L1} and the frequency, (b) i_{L2} and the frequency, (c) i_{L0} and the frequency

frequency. During the set time for fault nature identification (0.55–0.75 s), the extracted frequencies of i_{L1} , i_{L2} and i_{L0} are 25.62, 25.62 and 45.35 Hz, respectively, which are consistent with the results in Table 1. The criterion is satisfied and thus the fault is identified as a transient fault.

5.2.2 Permanent faults: In the scenario, a permanent phase A to ground fault occurs with the fault resistance $R_f = 300 \Omega$. The fault point is 200 km away from the M-end of the line. The fault occurs at 0.45 s. The M-end and N-end breakers are tripped, respectively, at 0.5 and 0.55 s. The M-end shunt reactor mode currents and oscillation frequencies are exhibited in Fig. 7.

Seen from Fig. 7, before the circuit is open at both ends at 0.55 s, the power frequency is obvious in i_{L1} and i_{L2} . After the tripping at both ends, i_{L0} oscillates in one frequency, whereas i_{L1} and i_{L2}

**Fig. 7** M-end mode currents and the frequencies under a permanent phase A to ground fault(a) i_{L1} and the frequencies, (b) i_{L2} and the frequencies, (c) i_{L0} and the frequency

each contains two frequency components. During the set time for fault nature identification (0.55–0.75 s), the extracted frequencies of i_{L1} are 25.62 and 33.47 Hz, the extracted frequencies of i_{L2} are 25.60 and 33.46 Hz, and the extracted frequency of i_{L0} is 33.43 Hz, which are consistent with the results in Table 1. The criterion is not satisfied and thus the fault is taken to be permanent.

The simulations for other fault types are properly missed here due to limited space. In brief, they also demonstrate that the fault nature can be discriminated with the proposed scheme.

6 Conclusion

This paper has investigated the shunt reactor mode currents in terms of their oscillation frequencies after three-phase trip. In transient fault situations, the mode currents oscillate in only one

frequency. However, in permanent fault situations, the mode current frequencies are dependent on the fault types.

Based on the frequency characteristics, this paper has proposed a three-phase adaptive reclosure scheme, in which the fault is identified to be transient when 1-mode, 2-mode and 0-mode currents each oscillate in one frequency which is the natural frequency of the corresponding mode network.

The simulation results have shown that the proposed scheme is capable of distinguishing the fault nature using only local end current data. The validity of the scheme is hardly affected by the fault location and fault resistance.

7 Acknowledgment

This work was supported by the National Key R&D Program of China (grant no. 2016YFB0900603).

8 References

- [1] Adly, A.R., El Schiemy, R.A., Abdelaziz, A.Y.: 'An optimal/adaptive reclosing technique for transient stability enhancement under single pole tripping', *Electr. Power Syst. Res.*, 2017, **151**, pp. 348–358
- [2] Sadi, M.A.H., Hasan Ali, M.: 'Combined operation of SVC and optimal reclosing of circuit breakers for power system transient stability enhancement', *Electr. Power Syst. Res.*, 2014, **106**, pp. 241–248
- [3] Ge, Y.Z., Sui, F.H., Xiao, Y.: 'Prediction methods for preventing from single-phase reclosing on permanent fault', *IEEE Trans. Power Deliv.*, 1989, **4**, pp. 114–121
- [4] Khodadadi, M., Noori, M.R., Shahrtash, S.M.: 'A noncommunication adaptive single-pole autoreclosure scheme based on the acusum algorithm', *IEEE Trans. Power Deliv.*, 2013, **28**, pp. 2526–2533
- [5] Luo, X.H., Huang, C., Jiang, Y.Q., *et al.*: 'Adaptive single-phase reclosure scheme for transmission lines with shunt reactors based on current inner product', *IET Gener. Transm. Distrib.*, 2017, **11**, pp. 1770–1776
- [6] Li, Y.L., Li, B., Huang, Q., *et al.*: 'The study of three-phase adaptive reclosure based on carrier channel and signal transmission', *Proc. Chin. Soc. Electr. Eng.*, 2004, **24**, pp. 74–79
- [7] Li, Y.L., Li, B.T.: 'Identification of three-phase permanent or temporary fault at transmission lines with shunt reactors', *Proc. Chin. Soc. Electr. Eng.*, 2010, **30**, pp. 82–90
- [8] Lin, D., Wang, H.F., Lin, D.Y., *et al.*: 'An adaptive reclosure scheme for parallel transmission lines with shunt reactors', *IEEE Trans. Power Deliv.*, 2015, **30**, pp. 2581–2589
- [9] Liang, Z.F., Suonan, J.L., Song, G.B., *et al.*: 'Discrimination of permanent faults for three-phase autoreclosing based on model identification', *Autom. Electr. Power Syst.*, 2010, **34**, pp. 81–85
- [10] Liang, Z.F., Suonan, J.L., Song, G.B., *et al.*: 'Permanent faults identification method for three-phase autoreclosing based on capacitance parameter', *High Volt. Eng.*, 2011, **37**, pp. 916–922
- [11] Suonan, J.L., Liang, Z.F., Song, G.B., *et al.*: 'Permanent faults identification for three-phase autoreclosure on transmission lines with shunt reactors'. 2011 IEEE APAP, Beijing, China, October 2011
- [12] Shao, W.Q., Zhang, W.N., Liu, Y.L., *et al.*: 'An improved scheme for the detection of permanent and transient earthed faults in reactor-compensated transmission lines'. 2015 IEEE Power and Energy Society General Meeting, Denver, CO, USA, July 2015
- [13] Liang, Z.F., Suonan, J.L., Kang, X.N., *et al.*: 'Permanent faults identification using oscillation frequency for three-phase reclosure on transmission lines with shunt reactors', *Proc. Chin. Soc. Electr. Eng.*, 2013, **33**, pp. 124–130
- [14] Dantas, K.M.C., Neves, W.L.A., Fernandes, D.: 'An approach for controlled reclosing of shunt-compensated transmission lines', *IEEE Trans. Power Deliv.*, 2014, **29**, pp. 1203–1211
- [15] Yang, L.M., Jiao, Z.B., Kang, X.N., *et al.*: 'A novel matrix pencil method for real-time power frequency phasor estimation under power system transients'. 12th IET Int. Conf. Developments in Power System Protection, Copenhagen, Denmark, April 2014